02

Experimental and theoretical studies of the ion-pair and valence states of the NeICl van der Waals complexes

© I.I. Martynov, S.A. Poretsky, A.M. Pravilov, M.M. Sivokhina

Department of Physics, Saint Petersburg State University, SPbSU,
St. Petersburg, Russia

e-mail: a.pravilov@spbu.ru

Received: November 12, 2024
Revised December 23, 2024
Accepted December 25, 2024

Experimental and theoretical studies of the T-shaped NeICl van der Waals (vdW) complexes in the ion-pair (IP) $E0^+$, $D'2$, $\beta 1$ and valence $A1$ states as well as the NeICl($A1$, υ_A, $n_A \leftarrow X0^+$, $\upsilon_X = 0$, n_X and β_1, υ_β, n_β/E_0^+, υ_E, $n_E \leftarrow A1$, υ_A, n_A) optical transitions have been carried out (n_i are vdW modes). We have measured NeICl(IP, $\upsilon_{IP} = 0$,$n_{IP} \rightarrow$ valence states) luminescence spectra and their excitation spectra. Binding energies of the states have been determined. The NeICl(IP, $\upsilon_{IP} = 1$, $n_{IP}) \rightarrow \mathrm{Ne} + \mathrm{ICl}(E, D', \beta)$ decay has been also studied. The intermolecular diatomic-in-molecule perturbation theory first order (IDIM PT1) method have been utilized to construct potential energy surfaces (PESs) for the complex valence, and IP states. Calculated spectroscopic characteristics of the NeICl E, β and valence states are similar to experimental ones. We calculated energies of the vdW mode and the action NeICl(A, υ_A, $n_A \leftarrow X0^+$, $\upsilon_X = 0$, n_x) as well as excitation NeICl(E, $\upsilon_E = 0$, $n_E \leftarrow A$, 13, n_A), NeICl(β, $\upsilon_\beta = 0$, $n_\beta \leftarrow A$, 13, n_A) spectra. Calculated excitation and action spectra describe the principal features of experimental spectra. We achieved satisfactory descriptions of the NeICl(E, $0 \rightarrow X$), NeICl(D', $0 \rightarrow A'$) and NeICl(β, $0 \rightarrow A$) luminescence spectra using Heidelberg MCTDH method, also.

Keywords:

DOI: 10.61011/EOS.2025.02.61016.7319-24

Introduction

Perturbations of diatomic molecule electronically excited bound states are one of the prime problems of chemical physics and molecular spectroscopy [1]. The complexes, containing rare gas atom and diatomic molecule bonded due to the van der Waals (vdW) interaction, are the simplest system to study and, on the other hand, are convenient model objects for acquiring a knowledge of more complex systems, to study many-body physics.

The study of intermolecular perturbations in optically populated vdW complexes can be facilitated by using dihalogens, X_2, and interhalogens, XY, as model systems. Therefore, the rare gas-X_2 and rare gas-XY vdW complexes in valence, $\mathrm{RgX_2}(B0_u^+)$, $\mathrm{RgXY}(A1, B0^+)$, states and $\mathrm{Rg} + \mathrm{X_2}(B)$ collision-induced non-adiabatic transitions, CINATs, have been studied since 1976 (see Refs. 1–3 and references).

Polarizability which is responsible for the dispersion interaction between Rg atom and dihalogen (interhalogen) in the complex seems to be significantly lower for the ICl molecule compared with the I_2. However, ICl has a permanent dipole moment (1.207 D for the X [4]), which is responsible for induction, dipole–induced dipole interaction. Potential energy surfaces (PESs) of the HeICl and ArICl have local minima with similar well depths at T-shaped and linear configurations.

Theoretical *ab initio* calculations were performed for the NeICl in the X [3] and B [5] state. For the ground state, it was shown that NeICl(X) state PES has three minima at linear (NeICl, binding energy $D_e = 106.8\,\mathrm{cm^{-1}}$), near T-shaped ($D_e = 84.79\,\mathrm{cm^{-1}}$), and antilinear (ICl-Ne, $D_e = 76.74\,\mathrm{cm^{-1}}$) configurations. O. Roncero *et. al.* [5] built PES of the NeICl(B) state using pairwise potentials. It was shown that there is the only one minimum located in the bent configuration ($\Theta_e = 140^\circ$) with the Ne atoms towards Cl end of ICl.

Experimentally ground $X0^+$ and excited, $B0^+$, $A1$ states were studied for the RgICl and RgIBr in the literature, Rg = He, Ne [6–11]. Using the LIF and pump-probe spectroscopy, assignments of the observed bands have been made and the binding energies of the ground and excited states have been estimated (see discussion in Subsection IV.2 of the paper). However, there is discrepancy between estimations of the binding energies.

D.B. Strasfeld et al [8] studied NeICl(B, $2 - X$, 0) transition. They observed series of bands and assigned them to transitions in different conformers. They attributed a single strong band as a transition in the T-shaped complex, and progression of bands as the transition in the linear NeI35Cl one.

$\mathrm{RgI_2}$(IP) vdW complexes have well depth significantly larger as those in the valence electronic states. Giant transition dipole moments between IP states sharing the same Ω quantum number lead to the increasing of the I_2 polarizability and increasing of the dispersion interaction (see Section 5 in Ref. 1). The ICl(IP) molecules have not such feature but their permanent dipole moment has to be

larger compared with that in the ground state, and the PES well depths of the RgICl(IP) complexes should be large than RgICl(valence) ones.

There are several works concerning to HeICl [11] and NeICl [10,12] complexes in the IP = $E0^+$, $D'2$, $\beta 1$ states. We have studied luminescence of the ArICl(IP,vIP) complexes and their decay products in a wide range of the vdW modes. The binding energies of the low vdW levels have been estimated [13–15]. All results show that the PESs of the IP states are deeper than that of the valence one. To determine the ArICl(β) binding energy, we assumed that the permanent dipole moment of the ICl(β) molecule is equal to 4 D [15].

Excited valence state RgX_2, RgXY complexes undergo fast vibrational and electronic predissociation (VP and EP, respectively). The NeICl(A) complex was found to have a long lifetime $\tau = (3 \pm 2)$ ns for $v_A = 14$ [6] much higher than usual ones for valence complex states (see Sect. 6 in [2] and references). However, lifetimes of the IP low lying vdW states are much longer. The NeICl(IP), IP = $E0^+$, $D'2$, and $\beta 1$ complexes were studied by T.A. Stephenson et al. [10]. They found luminescence of the ICl(IP) molecules after population of the mutual perturbed NeICl(E, $v_E = 0-4$) complex. Because populated vibrational levels lie below any dissociation limits of the IP states, no VP or EP mechanisms are available. They suggested that the origin of the observed luminescence is emission of the NeICl(IP) itself, that means at least comparable rates of the radiative and nonradiative decay process.

We determined the lifetime of the $NeI_2(E, 0)$ complex with the value $\tau = 8$ ns due to the complex luminescence and EP [16]. For the ArICl(E, 0) complex the measured lifetime $\tau = 20.3 \pm 1.0$ ns is close to one for free ICl(IP) molecules (radiative lifetimes of the free ICl(E, 0, β, 0, and D', 0) are 22.6(2), 22.6(2) and 14.8(1) (units, ns), respectively) [13]. We explain this value by significant coupling of different „diabatic“ E, β and D' states. It is to be expected the same behavior of the NeICl(IP) complexes. However, the lighter Ne atom should not initiate strong coupling of the IP states, and resonance effects should exhibit various coupling of different vdW levels. Therefore, variations of the lifetimes of different vibrational levels is expected to be observed in the NeICl complex.

In this paper, theoretical and experimental studies of the NeICl(IP, v_{IP}, n_{IP}) at energies lower than the NeICl(E, $v_E = 0$, n_E) dissociation limit are presented. In this energy range, NeICl(IP, $v_{IP} = 0$, n_{IP}) VP and EP is unavailable (see Subsection IV.2), and the NeICl(IP, v_{IP}, n_{IP}) luminescence can be observed, only [13,14]. Furthermore, excitation and luminescence spectra have also been measured in the energy range higher than the NeICl(E, $v_E = 0$, n_E) decay limit where the complex VP and EP are possible.

The first order intermolecular diatomic-in-molecule perturbation theory (IDIM PT1) method [17] is utilized to construct NeICl(A, A' and E, β, D') state PESs. Calculated binding energies of the T-shaped NeICl(A, and E, β) states agree well with experimental ones. Calculated excitation and action spectra describe the principal features of experimental spectra. We achieved satisfactory descriptions of the NeICl(E, 0, $n_X \rightarrow X$), NeICl(D', 0, $n_{D'} \rightarrow A'$) and NeICl(β, 0, $n_\beta \rightarrow A$) luminescence spectra using Heidelberg MCTDH method, also. These features are supporting the results of calculation.

The complexes containing Ar and Kr atoms are sufficiently difficult for analysis. These heavy atoms perturb all IP states resulting in their strong coupling do not allow to analyze structure of the states in details. On the other hand, well depths of the complexes with light He atom are low and do not have many vibrational levels. Therefore, HeICl complex has too simple structure in order to figure out PES features in detail. This work shows advantages of the NeICl complex which allows to build detailed PES of the valence and IP states. We have successfully developed a simple but suitable theoretical model.

The paper is organized as following: Methods and procedures utilized in experiments and analysis of experimental data are described in Section II. In Subsection III.1, 2, results of calculations of the complex valence and IP states PESs, their wavefunctions and some spectroscopic characteristics are discussed. An overview of experimental pump-probe and excitation spectra is described in Subsection IV.1. Subsection IV.2 is devoted to direct experimental determination of the complex state binding energies. Comparison of the calculated and experimental pump-probe and excitation spectra is carried out in Subsection IV.3. Subsections IV.4 is devoted to analysis of the luminescence spectra of the NeICl(IP) complexes in the energy range lower than their decay limits. Comparison of the experimental NeICl(IP) complex luminescence spectra with those calculated using Heidelberg MCTDH method is carried out in Subsection IV.5. Subsections IV.6 is devoted to analysis of the luminescence spectra, population and decay of the NeICl(IP) complexes in the energy range higher than their decay limits. In Section V, conclusions are given.

1. Experiment and analysis of experimental data

To study the NeICl valence and IP states spectroscopic characteristics we utilized a set of methods described in Refs. [13–16,18–26].

To prepare and stabilize NeICl(X) we utilized pulsed supersonic jet expansion. The He(99%) + Ne(1%) mixture ($p_{He} = 10-20$ atm) passed over the bubbler filled with mixed ICl and a teflon fillings, $t \approx 10°$C. Two counter-propagating temporally overlapped unfocused TDL90 laser beams crossed the molecular beam at the $x = (10 \pm 1)$ mm distance from the nozzle with axisymmetric nozzle diameter $D = 0.8$ mm, so $x/D \approx 12.5$. The two-step two-color NeICl NeICl (IP, $v_{IP} = 0$, $n_{IP} \overset{h_2}{\leftarrow} A$, $n_A \overset{h\nu_1}{\leftarrow} X$, 0, n_X). scheme was realized.

To distinguish quantum numbers of the populated NeICl(E, v_E/β, v_β) and NeICl(A, v_A) vibrational levels and n_E, n_β, n_A vdW modes, luminescence excitation spectra at selected λ_1, λ_{lum} as well as action spectra at selected λ_2, λ_{lum} were measured. We also studied pump-probe spectra (v_2 is fixed at the ICl(E, v_E/β, $v_\beta \overset{hv_1}{\leftarrow} A$, v_A) transitions and v_1 is scanned). Luminescence spectra of the NeICl(IP, v, v_{IP}, n_{IP}) complexes as well as NeICl(IP, v_{IP}, n_{IP}) VP and EP products have also been measured. The measurements procedures are reported in Refs. [1,13–16,18–29]. Temporal behaviors of the NeICl(IP, v_{IP}, n_{IP}) and ICl(IP, v_{IP}) luminescence intensities were also measured.

We used the $I^{35}Cl$, $I^{37}Cl$ spectroscopic constants, and RKR curves from Refs. [30,31] (A, X states), [32–35] (E, D', β). $NeI^{35}Cl$ isotopomer was studied.

2. Theoretical

In this paper, we used the approaches described in our previous work for the ArICl and HeICl vdW complexes [15,26].

2.1. The NeICl($X0^+$) state PES, wave functions and spectroscopic characteristics

The NeICl($X0^+$) state PES reproduced based on results of *ab initio* calculation carried out in Ref. [3] is shown in Fig. SD1. Fig. 1, *a* shows a comparison of the minimal energy path (MEP) of the NeICl(X) PES calculated in this work and in Ref. [3].

They coincide practically. The vdW binding energies and wavefunctions of the NeICl(X) state vdW levels are determined using the WavePacket software package in the Matlab environment [36]. In this problem, using the aforementioned calculation package, the stationary Schr.dinger equation is solved. Using the discrete variable representation (DVR) for R and θ coordinates [37], the equation is transformed into an eigenvalue problem. This equation is solved by direct diagonalization of the Hamiltonian matrix, resulting in calculated eigenvalues of the Hamiltonian and wave functions in a given coordinate space, the squares of which are usually interpreted as probability densities (see details in Ref. [15,26]). Positions of the $n_X = 0-3$ vdW levels obtained in this work are similar to those in Ref. 3 (see Table 1) since they have been calculated using NeICl(X) state PES of R. Prosmiti et al [3].

The calculated values of the NeICl(X) state spectroscopic parameters are presented in Table 1. The X state experimental and calculated binding energies differ significantly.

Plots of the $J = 0$ $NeI^{35}Cl$ probability amplitudes for the $n_X = 0-2$ vdW modes of the $NeI^{35}Cl$(X, $v_X = 0$) state and the same $NeI^{35}Cl$(A, 0, β, 0 and E, 0) vdW modes are given in Fig. 2.

2.2. The NeICl($A1$, $\beta1$ and $E0^+$) state PESs, wavefunctions, and spectroscopic characteristics

The IDIM PT1 method [17] was utilized to construct the NeICl(A, β and E) state PESs. The detailed PES building procedure and obtained formulae are described in our previous works [15,26]. The NeICl(A, β and E) state PESs and MEPs obtained are given in Fig. SD2 and Fig. 1, *b, c, d*, respectively. The van der Waals binding energies (Table 1) and wavefunction probability amplitudes of the NeICl(A, β and E) state vdW levels (Fig. 2) are determined by the way described in previous Section.

Importantly, unlike the HeICl system [26], which necessitated further modifications to the PESs, the NeICl system only required the inclusion of the induction interaction within the Ne-$Cl^-(^1\Sigma^+)$ pair potential [42] using a correction from Ref. [43].

$$V^*(R) = V(R) - f^*(R)\left(\frac{1}{2}\frac{\alpha_1}{R^6} + \frac{1}{2}\frac{\alpha_2}{R^8}\right),$$

where α_1 and α_2 are the dipole and quadrupole polarizabilities of the Ne atom, respectively, and $f^*(R)$ is a switching function.

$$f^*(R) = \frac{1}{2}[1 + \tanh(1 + \delta R)].$$

The values of α_1 and α_2 for Ne-$I(\Pi^3, {}^3\Sigma^-)$ were calculated from the pair potentials from Ref. 44, following the methodology outlined in Ref. 15.

$$\alpha_1\left(\text{Ne} - \text{I}(^3\Pi, {}^3\Sigma^-)\right) = -0.44 \cdot 10^5,$$

$$\alpha_2\left(\text{Ne} - \text{I}(^3\Pi)\right) = 0.15 \cdot 10^6,$$

$$\alpha_2\left(\text{Ne-I}(^3\Sigma^-)\right) = -0.13 \cdot 10^6.$$

For Ne-$Cl^-(^1\Sigma^+)$, the values of α_1 and α_2 were determined by optimizing the agreement with experimental data:

$$\alpha_1\left(\text{Ne-Cl}^-(^1\Sigma^+)\right) = -0.35 \cdot 10^5,$$

$$\alpha_2\left(\text{Ne-Cl}(^1\Sigma^+)\right) = 0.114 \cdot 10^6.$$

The calculated values, obtained without significant modifications to the PES construction, exhibit good agreement with experimental data.

3. Results and discussion

3.1. Overview of the pump-probe and excitation spectra

The ICl($E, 0 \rightarrow X$ and $\beta, 0 \rightarrow A/D'$, $0 \rightarrow A'$) luminescence pump-probe spectra for pumping in the vicinity of the ICl(A, $v_A = 13 \overset{hv_1}{\leftarrow} X$, 0) transition and probing at the ICl(β, $v_\beta = 0 \rightarrow A$, 12) transition, $v_2 = 23190.0\,\text{cm}^{-1}$ is given in Fig. 3.

One sees bands corresponding to ICl(A, $13 \leftarrow X$, 0), T-shaped NeICl(A, 13, $n_A \leftarrow X$, 0, n_X), T-shaped Ne_2ICl(A,

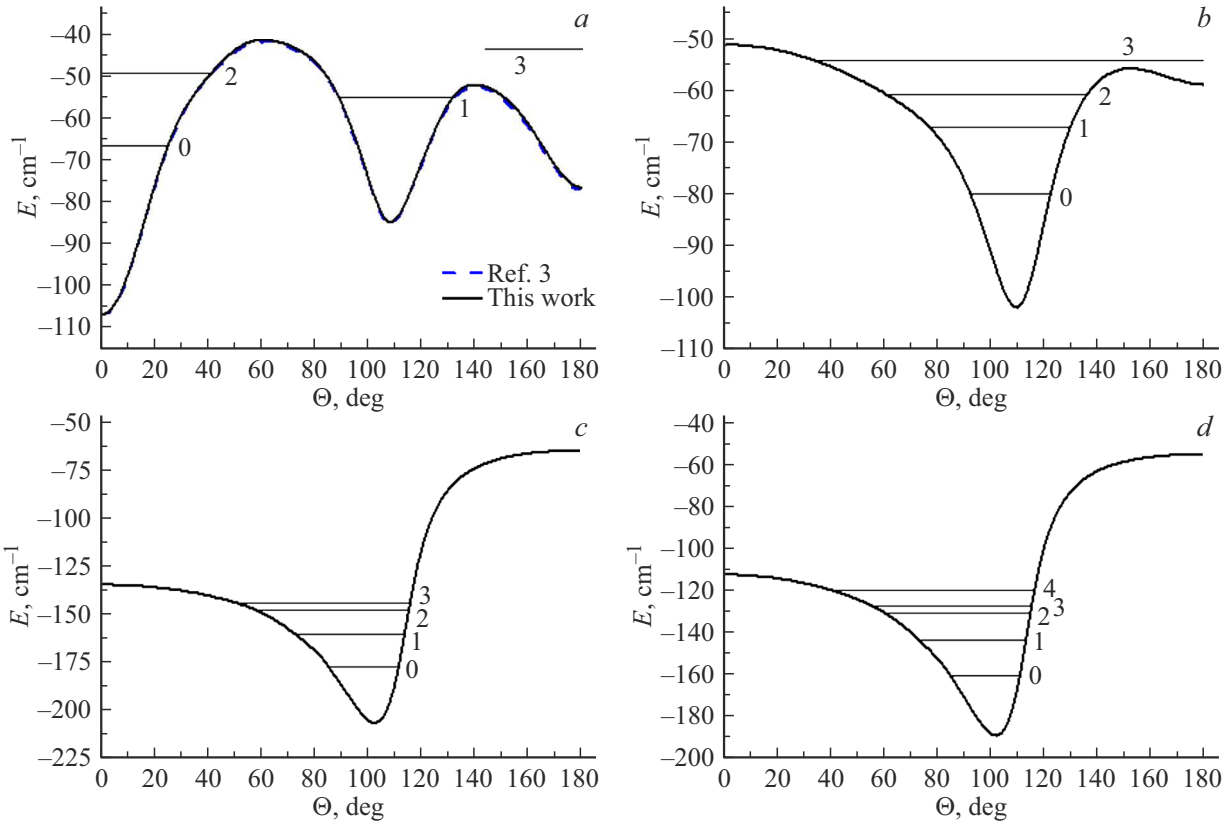

Figure 1. Minimum energy paths on the NeICl(X) (a), NeICl(A) (b), NeICl(β) (c), and NeICl(E) (d) obtained in this work and given in Ref. 3 Positions of low vdW levels are shown.

$13 \leftarrow X,\ 0$), and T-shaped $Ne_3ICl(A,\ 13 \leftarrow X,\ 0)$ transitions. Their assignment is made in accordance with the band shift rule (see [45] and references). The $ICl(A,\ 13 \leftarrow X,\ 0)$ band arises from $ICl(A,\ 13) \overset{He}{\rightarrow} ICl(A,12)$ collisions which are still occurring in the observation region. We have observed similar processes many times. The $NeICl(A,\ 13,\ n_A \leftarrow X,\ 0,\ n_X)$ band occurs due to the $NeICl(A,\ 13) \rightarrow Ne + ICl(A,12)$ VP accompanied by transitions to the mixed states $ICl(\beta,\ v_\beta = 0,\ v_E = 0 \overset{hv_2}{\leftarrow} A,\ 12)$ and their luminescence. The $Ne_2ICl(A,\ 13 \leftarrow X,\ 0)$ band can be observed (a) due to the $Ne_2ICl(\beta,\ v_\beta = 2,\ v_E = 2,\ n_\beta,\ n_E \overset{hv_2}{\leftarrow} A,\ 13)$ accompanied by VP, EP and luminescence, (b) $Ne_2ICl(A,\ 13) \overset{hv_2}{\leftarrow} Ne + NeICl(A,\ 12)$ VP accompanied by the transitions to the mixed states, $NeICl(E,\ D',\ \beta,\ v = 0 \overset{hv_2}{A},\ 12)$, and their luminescence. Similar processes can take place in the Ne_3ICl cluster.

We have observed the $NeICl(A,\ v_A = 13,\ n_A = 0 \overset{hv_1}{X},\ 0,\ n_X = 1)$ transition only, in the experiments. All our attempts to detect the linear NeICl(A) vdW complexes were fruitless (see Fig. SD3). As it turned out, the wide $v_1^{max} \approx 15\,965\,cm^{-1}$ band belongs to the linear HeICl(A) vdW complexes.

The excitation spectra of the $NeICl(E,\ v_E = 0,\ n_E \rightarrow X)$ and $NeICl(\beta,\ v_\beta = 0,\ n_\beta \rightarrow A/D',\ v_{D'},\ n_{D'} \rightarrow A')$ luminescence for the T-shaped configuration are given in Fig. 4.

One sees that all the bands in Fig. 4 lie in the energy range lower than the $NeICl(\beta,\ 0,\ n_\beta)$ dissociation limit, $23129\,cm^{-1}$, and all the bands with the exception of those at $v_2 > 23\,082\,cm^{-1}$, lie in the energy range where $NeICl(E,\ 0,\ n_E,\ D',\ 0,\ n_{D'})$ decay is impossible. Therefore, luminescence of the $NeICl(E,\ 0,\ n_E,\ D',\ 0,\ n_{D'},\ \beta,\ 0,\ n_\beta)$ complexes themselves is only possible in the $v_2 < 23\,082\,cm^{-1}$ energy range.

The intensities of excitation bands in Fig. 4 corresponding to the $NeICl(\beta,\ 0,\ n_\beta \rightarrow A/D',\ 0,\ n_{D'} \rightarrow A')$ luminescence are low in the $v_2 < 22950\,cm^{-1}$ energy range. The $NeICl(E,\ 0,\ n_E \rightarrow X)$ luminescence is the strongest here, and one may assign the $v_2 = 22922.8$ and $22941.5\,cm^{-1}$ bands as belonging to the $NeICl(E,\ 0,\ n_E = 0,\ 1 \leftarrow A,\ 13,\ n_A = 0)$ transitions. Results of calculations and the $NeICl(E,\ 0,\ n_E = 0)$ luminescence spectrum confirm this statement (see Sects. IV.3–IV.5).

The first excitation bands at which the $NeICl(\beta,\ 0,\ n_\beta \rightarrow A/D',\ 0,\ n_{D'} \rightarrow A')$ luminescence becomes strong occur at the $v_2 > 22950\,cm^{-1}$ energy range, and the $v_2 = 22951.8$ and $22966.6\,cm^{-1}$ bands may be assigned to the $NeICl(\beta,\ 0,\ n_\beta = 0,\ 1 \leftarrow A,\ 13,\ n_A = 0)$ transitions. Results of calculations and the $NeICl(\beta,\ 0,\ n_\beta \rightarrow A/D',\ 0,$

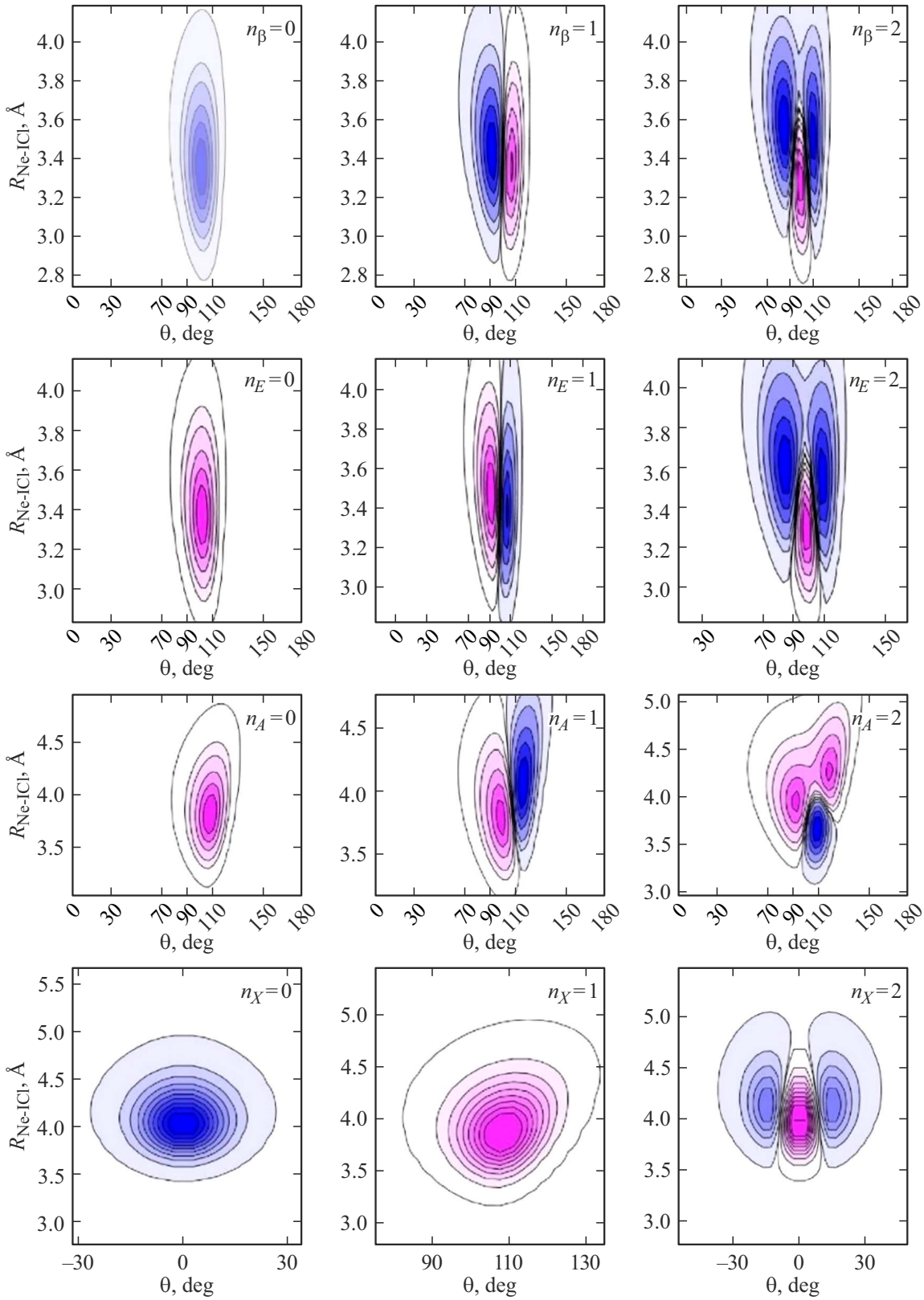

Figure 2. Plots of the $J = 0$ $HeI^{35}Cl$ probability amplitudes for the $n_i = 0{-}2$ vdW modes of the $NeI^{35}Cl(X, \upsilon_X = 0)$, $NeI^{35}Cl(A, \upsilon_A = 13)$, $NeI^{35}Cl(\beta, \upsilon_\beta = 0)$, and $NeI^{35}Cl(E, \upsilon_E = 0)$ states.

Some spectroscopic parameters (experimental and calculated), potential well depths D_e (cm^{-1}) and respective equilibrium coordinates R_e (Å) and Θ_e, binding energies D_0 (cm^{-1}) of the NeICl complexes in the near-T-shaped ($\Theta \approx 90°$) and linear ($\Theta \approx 0°$) configurations (see Sect. 4.2)

State	Reference	Linear, $\theta = 0$			Near T-shaped		
		D_e	D_0	R_e	D_e	D_0	R_e/θ_e
$X0^+,0$	[3]	106.8	76.19	3.96	84.79	62.59	3.78/109.1
	[8]		84(1)				
	[38]					70(5)	
	[39]					70	
	[12]					48.2(5)	
	This work, calculated	106.8	79.62	3.96	84.7	64.86	3.77/109.1
	Experiment		~ 100			84(1)	
$A1$	[10]					$\leq 60^{(1)}$	
	[12]		48.2(5)			43–45	
	[40,41]					41–45	
	[38]					$62–65^{(2)}$	
	This work, calculated				101.8	$80.37^{(3)}$	3.7/109.4
	Experiment					$80(1)^{(3)}$	
$\beta 1$	This work, calculated				205.4	178.06	3.3/102.5
	Experiment					178(1)	
$E0^+$	[12]					87.6(8)	
	This work, calculated				189.1	161.03	3.3/102.5
	Experiment					161(1)	

Note. (1) $v_A = 14$,
(2) $v_A = 23$,
(3) $v_A = 13$.

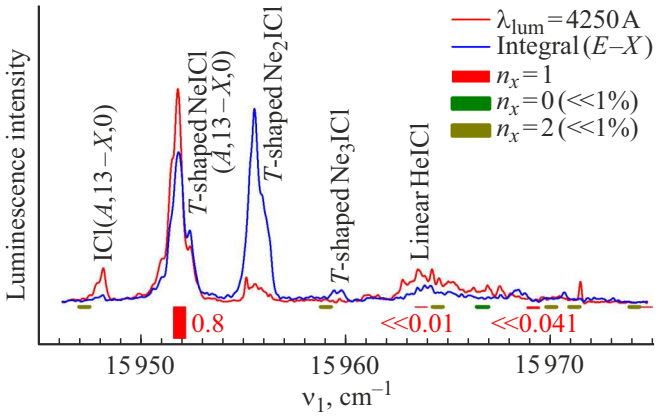

Figure 3. The pump-probe spectra of the ICl($E, 0 \to X$ and $\beta, 0 \to A/D'$, $0 \to A'$) luminescence in the vicinity of the ICl($A, v_A = 13 \overset{h\nu_1}{\leftarrow} X, 0$) transition and probing at the ICl($\beta, v_\beta = 0 \overset{h\nu_2}{\leftarrow} A, 12$) transition, $\nu_2 = 23\,190.0\,cm^{-1}$. Franck-Condon factors of the NeICl($A, v_A = 13, n_A \overset{h\nu_1}{\leftarrow} X, 0, n_X = 0, 1, 2$) transitions calculated using wave functions obtained in this work (see Fig. 2) are presented.

$n_{D'} \to A'$) luminescence spectra confirm this statement (see Sects. IV.3-IV.4).

Comparison of excitation spectra corresponding to the population of $v_{E,\beta} = 0, 1$ vibronic levels of the complexes is shown in Fig. 5.

The ICl(β, $1 - A$, $v_A = 13$) FCF is low, 0.0036. Therefore, the NeICl(A, $v_A = 12$, $n_A = 0$) level has been used as intermediate one for population of the HeICl(β, 1, n_β) complexes (unfortunately, FCF of the ICl(E, $1 - A$, $v_A = 12$) transition is also low, 0.004). One should note that NeICl(E, β, 1, $n_{E,\beta}$) complexes can undergo EP and VP.

Positions of the excitation band in Fig. 5 are similar but do not coincide. Differences lie in the $\Delta(\nu_1 + \nu_2) = 0–3.5\,cm^{-1}$; the $\Delta(\nu_1 + \nu_2) = 3.5\,cm^{-1}$ is the energy difference of the NeICl(β, $v_\beta = 0$, 1, $n_\beta = 0 \leftarrow A$, 13, $n_A = 0$) transitions. The ICl(β, $1 - \beta$, 0) energy difference is $169\,cm^{-1}$, and NeICl(β, $v_\beta = 1$, $n_\beta = 0$) binding energy should be $178\,cm^{-1}$ (see Table 1). Therefore, the NeICl(β, $v_\beta = 1$, $n_\beta = 0$) level, for example, lies a little below the NeICl(β, $v_\beta = 0$, n_β) dissociation limit and may be perturbed by a high NeICl(β, $v_\beta = 0$, n_β) levels.

Excitation spectra measured in Ref. [10] and this work are given in Fig. SD4. Positions of the NeICl($\beta \to A/D' \to A'$) bands in Fig. SD4, *a, b* are similar. As to the NeICl($E \to X$) bands, Stephenson *et al* did not observe them in the $\nu_1 + \nu_2 < 38\,940\,cm^{-1}$ spectral range due to the low signal-to-noise ratio, probably.

3.2. Determination of the NeICl state binding energies

Data on NeICl(X, A, E, β) state binding energies and their analysis are presented in Refs. [3,8,10,12,38.41]. In

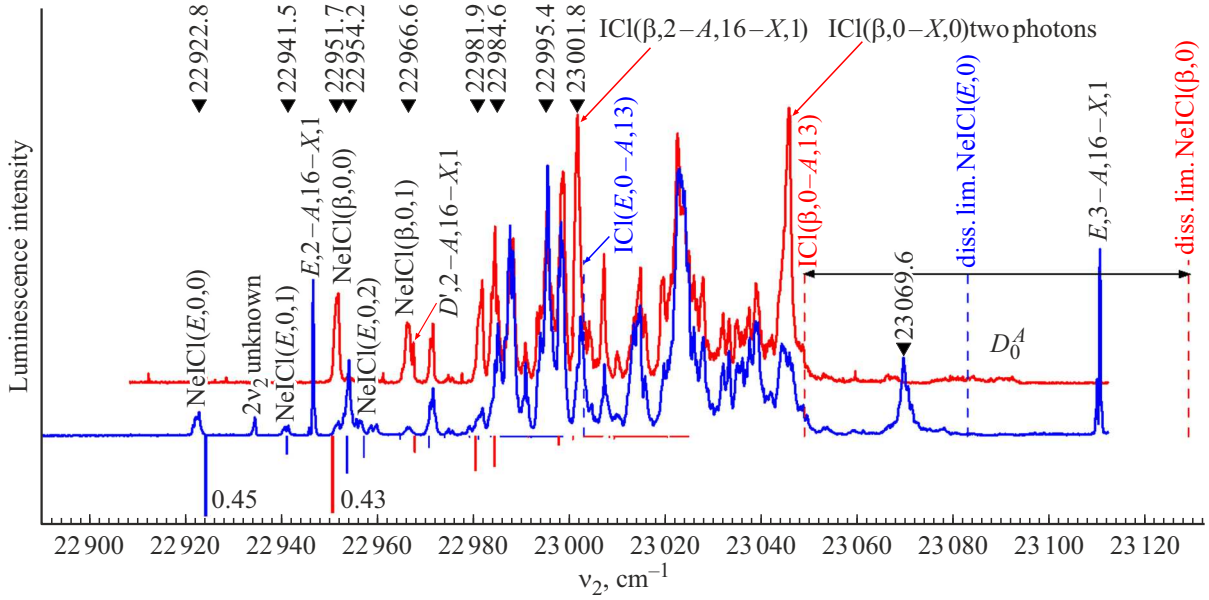

Figure 4. The NeICl(E, β, υ_E, $\beta = 0$, $n_{E,\beta} \leftarrow A$, 13, $n_A = 0$) excitation spectra of the luminescence measured in the $\lambda_{\text{lum}} = 3500-4000$ Å spectral range (blue line) and at $\lambda_{\text{lum}} = 4250$ Å (red line), $\nu_1 = 15951.8\,\text{cm}^{-1}$, T-shaped NeICl(A, 13, $n_A = 0 \leftarrow X$, 0, $n_X = 1$) transition. Positions of the bands at which luminescence spectra have been measured are marked by triangles. Dissociation limits of the NeICl(β,0) and NeICl(E, 0) complexes are marked, and calculated FCFs of the NeICl(E, $\upsilon_E = 0$, $n_E \leftarrow A$, 13, n_A), NeICl(β, $\upsilon_\beta = 0$, $n_\beta \leftarrow A$, 13, n_A) transitions are shown.

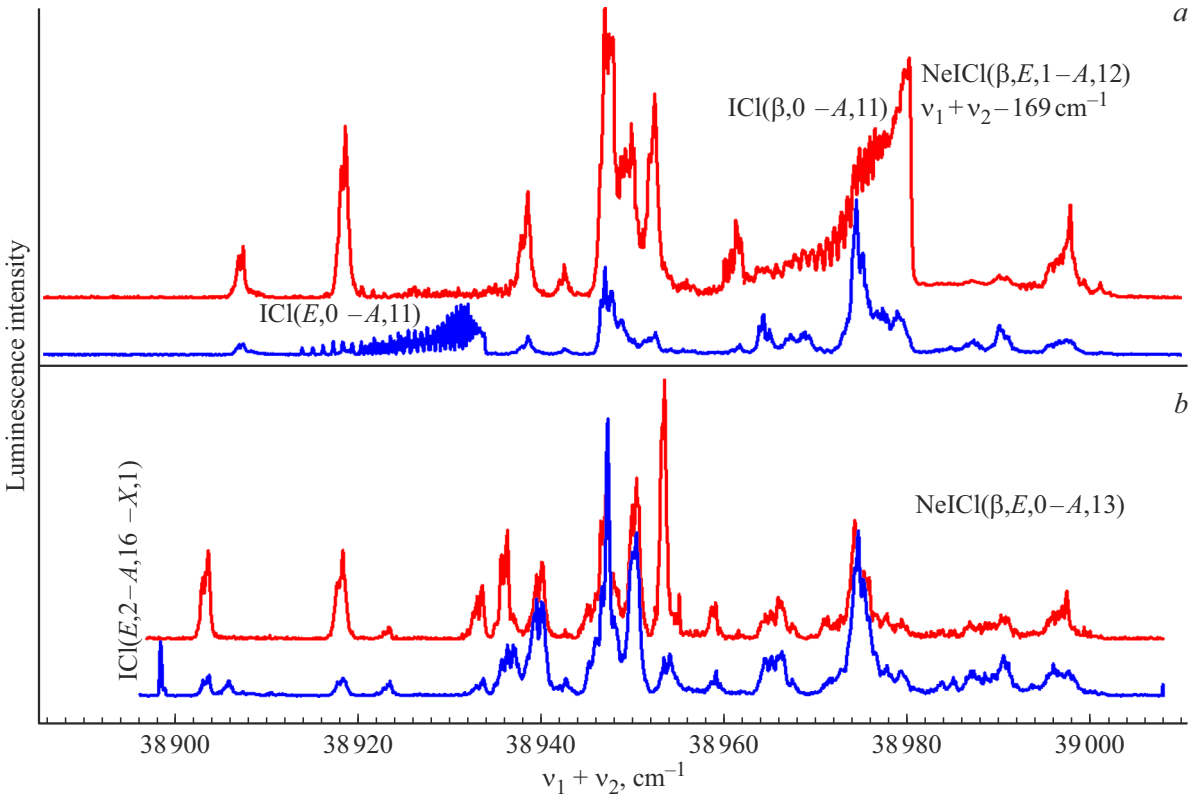

Figure 5. Excitation spectra of the luminescence measured in the $\lambda_{\text{lum}} = 3500-4000$ Å spectral range (blue line) and at $\lambda_{\text{lum}} = 4250$ Å (red line) using the NeICl(E, β, 1, $n_{E,\beta} \overset{h\nu_2}{\leftarrow} A$, $\upsilon_A = 12$, $n_A = 0 \overset{h\nu_1}{\leftarrow} X$, 0, $n_X = 1$), $\nu_1 = 15809.5\,\text{cm}^{-1}$ (a), and NeICl(E, β, 0, $n_{E,\beta} \overset{h\nu_2}{\leftarrow} A$, $\upsilon_A = 13$, $n_A = 0 \overset{h\nu_1}{\leftarrow} X$, 0, $n_X = 1$), $\nu_1 = 15951.8\,\text{cm}^{-1}$ (b) schemes. The ν_2 generation intensity is ~ 15 times lower than that of using in Fig. 4. The ICl(β, $1-\beta$, 0) energy difference, $169\,\text{cm}^{-1}$, is subtracted from the $\nu_1 + \nu_2$ value in the a panel.

all experimental works, the highest rotational levels of the ICl(A, v_A, J_A) states nascent in NeICl(A) VP, ICl(A, v_A, $J_A^{\max}$), were used for the determination of the ICl(A, v_A, J_A) state rotational excitation energy. Then the NeICl(X, A, E, β) binding energies were determined using the spectral shifts of the NeICl($E/\beta \leftarrow A$) and NeICl($A \leftarrow X$) transitions relative to those of a free molecule.

However, vibrational energy of the complex in VP releases also into kinetic energy of fragments recoil, and the energy of the NeICl(A, v_A, n_A) is equal to the sum of ICl(A, $v_A - 1$, $J_A^{\max}$) energy and the kinetic energy of the Ne + ICl(A, v_A, J_A) fragments (kinetic energy release, KER).[13] In the case of the ArICl(A, v_A, n_A) predissociation, $187\,\text{cm}^{-1} \le D_0^{A,v_A=13} \le 210\,\text{cm}^{-1}$ [13]. One sees that determination error of the NeICl(A, v_A, n_A) binding energy is large.

Therefore, we decided to carry out its direct measurement in the manner used in Ref. [8,45], i.e. to measure pump-probe, NeICl(A, 13, $n_A \leftarrow X$, 0, n_X) (pump), ICl(E, $0 \leftarrow A$, 13) (probe) spectra, and find the NeICl(A, 13, n_A) dissociation limit. We knew that NeICl(A, 13, $n_A \leftarrow X$, 0, n_X), ICl(E, $0 \leftarrow A$, 13) transitions had to exist, and $D_0^{A,v_A} \ge 60\,\text{cm}^{-1}$. Therefore, we used the Ne(5%) + He(95%) mixture and carried out measurements in large, $\nu_1 \approx 15940-16050\,\text{cm}^{-1}$ energy range. One sees in Fig. SD3 the bands corresponding to populations of the ICl(A, 13) free molecule, NeICl(A, 13, $n_A = 0$) T-shaped complex, Ne$_n$ICl(A, 13, $n_A = 0$), $n = 2$, 3 clusters, and HeICl(A, 13, $n_A = 1$) linear (free-rotor) complex. According to results of our calculations, the intensities of NeICl(A, 13, $n_A = 1$, $2 \leftarrow X$, 0, n_X) transitions are negligible (see Sect. IV.2).

One should discuss which, the T-shaped or linear (free-rotor) NeICl(X) complexes, corresponds to this threshold. Both linear NeICl(X, 0, $n_X = 0$) and T-shaped NeICl(X, 0, $n_X = 1$) complexes exist in a supersonic beam. One cannot observe ICl(A) luminescence and determine its rotational temperature due to large ICl(A) radiative lifetime, $> 10^{-4}$ s (see Ref. [46]). Therefore, we decided to use ICl(X, 0) rotational temperature, $T_{\text{rot}} = 1.36(2)$ K, determined in Ref. [47] for HeICl in the conditions ($p_{\text{He}} = 18.5$ bar, $x/D = 11.9$) very similar to those used in our experiments ($p_{\text{He}} = 20$ atm, $x/D = 12.5$). Population of the NeICl(X,0) $n_X = 1$ (T-shaped) mode is exp(−15/5.4) less than that of $n_X = 0$ (linear) one (15 cm^{-1} and 5.4 cm^{-1} are NeICl(X, 0) and HeICl(X, 0) energy differences of the $n_X = 0$ and 1 modes, respectively) [11]. Therefore, NeICl(X, 0, $n_X = 1$) population is $\exp(-15/5.4) \cdot (0.37/0.65) = 0.036$ of that of NeICl(X, 0, $n_X = 0$) (0.65 and 0.37 are relative populations of the NeICl(X,0) $n_X = 0$ and 1 conformers at $x/D = 13$) [48]. Nevertheless, we have not observed the linear NeICl(A) conformer due to negligible FCFs of the linear NeICl(X, 0, $n_X = 0$) conformer transitions.

According to the results of our calculations, there is no minimum at the NeICl(A, 13, n_A) PES at linear configuration (see Fig. SD2), the $n_A \le 2$ vdW levels corresponds to the near T-shaped configuration (Fig. 1, b). The NeICl(A, 13, $n_A \ge 5 \leftarrow X$, 0, $n_X = 0$) transitions are of negligible probabilities due to large differences of R values corresponding to the NeICl(X, 0, $n_X = 0$) (3.97 Å) and NeICl(A, 13, $n_A \ge 5$) (~ 4.5 Å) states. Franck-Condon transition from the linear NeICl(X, 0, $n_X = 0$) ($R = 3.97$ Å) state occurs at the repulsive part of the NeICl(A, 13, n_A) PES lying much higher than the NeICl(A, 13, n_A) dissociation limit. Therefore, the $\nu_1 = 16032\,\text{cm}^{-1}$ threshold corresponds to the T-shaped configuration, and the NeICl(A, 13, $n_A = 0$) binding energy is equal to $D_0^{A,13} = 80(1)\,\text{cm}^{-1}$, $\sim 15\,\text{cm}^{-1}$ larger than determined earlier [10,12,38,40,41]. The NeICl(X, 0, $n_X = 1$) binding energy is equal to $D_0^{X,0,1} = 84(1)\,\text{cm}^{-1}$ since the ICl(A, 13) — NeICl(A, 13, $n_A = 0$) blue shift is 4 cm^{-1} and the linear NeICl(X, 0, $n_X = 0$) binding energy is $D_0^{X,0} \approx 100\,\text{cm}^{-1}$ (see Table 1, Fig. 6).

Energy level diagram for the NeICl(X, 0, $n_X = 1$, A, 13, $n_A = 0$, E, 0, $n_E = 0$, β, 0, $n_\beta = 0$) complexes calculated using the T-shaped NeICl binding energies, $D_0^{A,13} = 80(1)\,\text{cm}^{-1}$, $D_0^{X,0} = 84(1)\,\text{cm}^{-1}$, determined, and other experimental data obtained in this work is given in Fig. 6.

One should note that Ne + ICl(E, 0) dissociation limit lies 161 cm^{-1} higher than the NeICl(E, 0, $n_E = 0$) state. Dissociation limits of the T-shaped NeICl(D', 0) and NeICl(β, 0) complexes are 1.4 cm^{-1} and 46.4 cm^{-1} higher (see Fig. 4, also). Therefore, NeCl(IP ,$v_{\text{IP}} = 0$, $n_{\text{IP}} = 0$) VP and EP is unavailable.

In principle, $\nu_1 > 16032\,\text{cm}^{-1}$ continuum can correspond to the Ne$_2$ICl(E, 0, n_E) → Ne + NeICl(E, 0, n_E) cluster dissociation. It is well known, however, that RgICl(E, 0, $n_E \to X$, v_X) luminescence bands are similar to those of ICl(E, 0, $n_E \to X$, v_X) but are shifted relative to the latter (see Refs. [2,26] and references). The luminescence spectrum measured at the continuum coincides with the ICl(E, $0 \to X$) one (Fig. SD5).

The data on the NeICl(X, A, E) binding energies obtained in this work differ significantly from those given in Refs. [3,8,10,12,38–41] (see Table 1). We have to discuss these contradictions.

D.B. Strasfeld et al [8] have measured LIF, I^{35}Cl(B, $v_B = 2 \to X$, v_X) and pump, NeI^{35}Cl(B, $v_B = 2 \to X$, v_X), probe, I^{35}Cl(E, $v_E = 11 \leftarrow B$, $v_B = 2$), spectra at different $x/D = 7.5-25$ (x is the downstream distance and D is the nozzle diameter). They have observed the single strong band corresponding to the T-shaped complex, and progression corresponding, as authors believe, to the linear NeI^{35}Cl(B, $v_B = 2$) complexes in LIF spectra. Integral intensity of the T-shaped band is larger than total intensity of the linear bands. Besides, they observed continua in LIF and pump-probe spectra corresponding, as authors believe, to transitions of the linear NeI^{35}Cl(X, $v_X = 0$) conformer to above the Ne + I^{35}Cl(B, $v_B = 2$) asymptote.

The authors of Ref. [8] have affirmed that the continuum fluorescence intensity in the LIF spectra tracks with the linear progression intensity when x/D increase from $x/D = 7.5$ to 25. Therefore, observed results from transitions of the linear Ne–I^{35}Cl(X, 0) conformer.

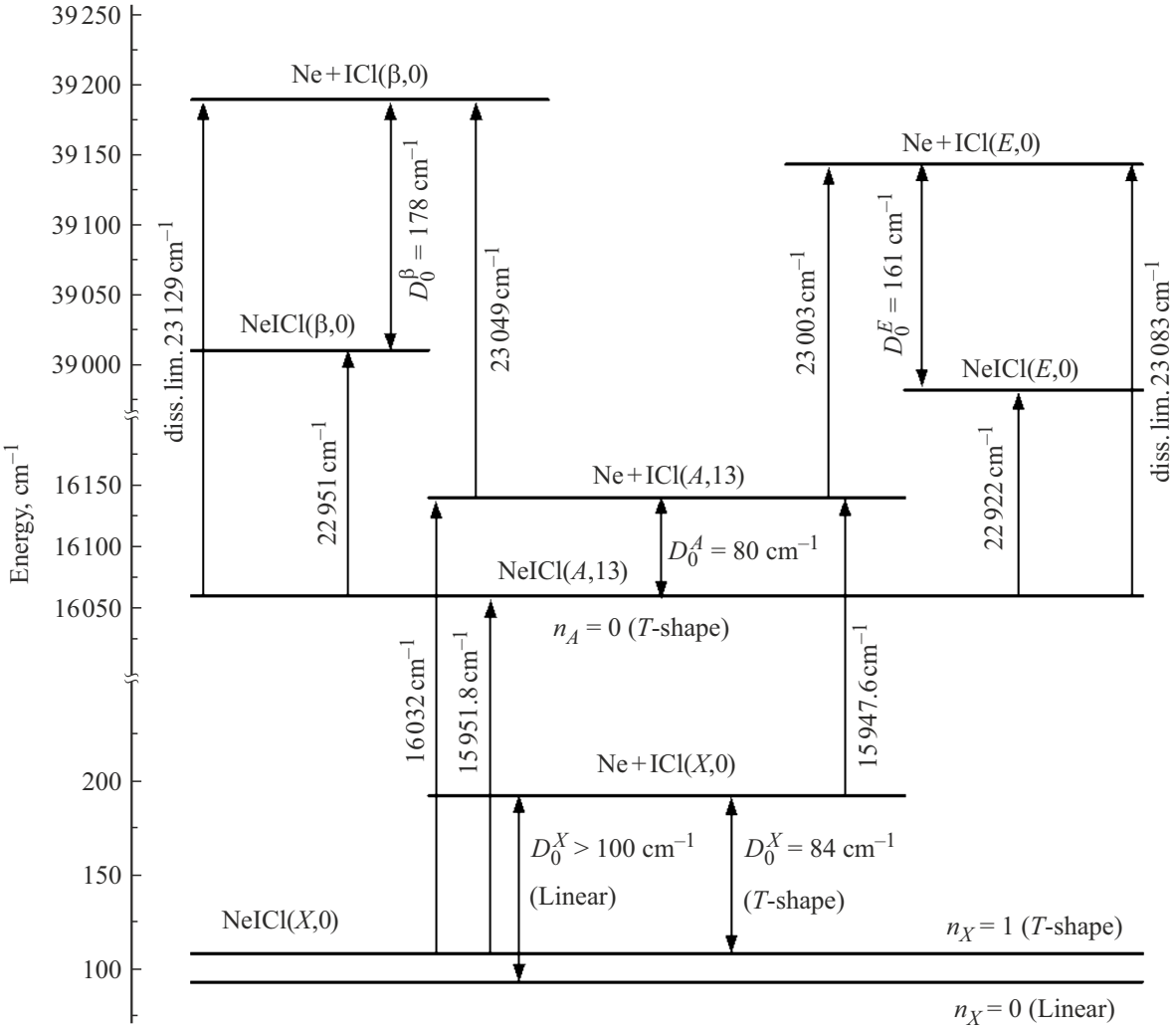

Figure 6. Energy level diagram for the NeICl(X, 0, n_X, A, 13, $n_A = 0$, E, 0, $n_E = 0$, β, 0, $n_\beta = 0$) complexes.

There are serious doubts about the correctness of the assignment the progression and continua to the linear conformer.

1. According to the calculations of O. Roncero et al [5], there is the only one minimum at NeICl(B, υ_B) PES, and it is located in the bent configuration, $D_e = -67\,\text{cm}^{-1}$, $R_e = 4.95$ Å, $\Theta_e = 140^\circ$ (the Ne atoms towards Cl end of ICl). No minimum exists in the linear configuration, $\Theta = 0^\circ$, and bound-bound NeICl(B, $\upsilon_B = 2 \leftarrow X$, υ_X) transitions are impossible in the linear configuration.

2. One sees in Fig. 2 of Ref. [8] that the average ratio of the intensities of the linear conformer bands measured at a rotational temperature of 0.81 K to those of at 3.9 K is 1.8, while for the continuum this ratio is 1.4. If the continuum belongs to the linear conformer, these ratios should be the same.

3. We have measured the pump-probe, NeICl(A, 13, $n_A \leftarrow X$, 0, n_X) (pump), ICl(E, $0 \leftarrow A$, 13) (probe, $\nu_2 = 23003\,\text{cm}^{-1}$) spectrum, $\lambda_{\text{lum}} = 3500-4000$ Å, ICl($E \rightarrow X$) transition in wide, $15938-16051\,\text{cm}^{-1}$ spectral range (see Fig. SD3). If the continuum observed in our experiments belongs to the linear conformer, the continuum belonging to the T-shaped conformer has to start at $\sim (16032-15) = 16017\,\text{cm}^{-1}$. We have observed no continuum at $\nu_2 > 16017\,\text{cm}^{-1}$. There is only a weak continuum started at $\nu_1 = 15970\,\text{cm}^{-1}$ and corresponding to transitions in the HeICl complex. It should also be noted that, in the HeICl vdW complex. these two continua are observed [45], and the difference in the wave number of their appearance is equal to $3\,\text{cm}^{-1}$, i.e., the difference in the binding energies of the linear and T-shaped conformers of NeICl(X) [3].

T.A. Stephenson et al [10] using the data of Ref. [41] (NeICl(A, $\upsilon_A = 23$)) and conception of Ref. [38] (see below) estimated the NeICl(A, $\upsilon_A = 14$) binding energy as $\leq 60\,\text{cm}^{-1}$.

K.C. Janda, C.R. Bieler [38] estimated the NeICl(X,0) binding energy as $70(5)\,\text{cm}^{-1}$ using the NeICl(A, $\upsilon_A = 23$) VP product rotational distribution obtained in Ref. [41].

J.I. Cline et al [39] proposed the T-shaped D_o(NeICI(X) $= 70\,\text{cm}^{-1}$ comparing the NeCl2 dynamics to those of NeICI.

J.C. Drobits, M.I. Lester [12] measured double resonance spectrum by promoting NeICl(X,0) to NeICl(A, $v_A = 12$, 14, 15) and probing NeICl(E, $v_E = 1 - A$, v_A) transition. They determined the NeICl(E, $v_E = 1$) binding energy as 87.6(8) after analysis of progression measured and then those of NeICl(X, 0) and NeICl(A, $v_A = 12$, 14, 15) using pump and probe blue shifts.

One sees in Table 1 that discrepancies of the binding energies obtained earlier are too large.

The authors of Ref. [40,41] believe that binding energies of the NeICl(A, $v_A = 11$, 14, 19, 23) complexes lies in the $D_0^{A,11-23} \approx 41-45\,\mathrm{cm}^{-1}$ range, whereas authors of Ref. [38] believe that $D_0^{A,23} = 62-65\,\mathrm{cm}^{-1}$. As to J.C. Drobits and M.I. Lester paper [12], their assignment of the bands and especially the dissociation limit in Fig. 4 of the paper questionable. The peak assignment by the author to continuum is too narrow to be a continuum (see Fig. SD3). We measured similar spectra (Figs. 4, 5), but we found two additional bands in the NeICl(E, β, $v_{E,\beta} = 0$, $n_{E,\beta} \leftarrow A$, 13, $n_A = 0$) excitation spectra of the luminescence, lying deeper, at $\nu_2 = 22922.8$ and $22941.5\,\mathrm{cm}^{-1}$ (Fig. 4). Moreover, no continua were observed in our spectra at $\nu_2 > (22922.8 + 87.6) = 23010.4\,\mathrm{cm}^{-1}$. Therefore, the values of NeICl(E, $v_E = 1$) binding energies, $87.6\,\mathrm{cm}^{-1}$, determined in Ref. [12] are underestimated.

As is mentioned above, we have not observed the linear conformer in the pump-probe spectra of the ICl(E, $0 \rightarrow X$ and β, $0 \rightarrow A/D'$, $0 \rightarrow A'$) luminescence in the vicinity of the ICl(A, $13 \overset{h\nu_1}{\leftarrow} X$, 0) transition and probing at the ICl(β, $v_\beta = 0 \overset{h\nu_2}{\leftarrow} A$, 13) transition (see Fig. SD3). According to our calculation, NeICl(A, 13, $n_A \geq 5 \leftarrow X$, 0, $n_X = 0$) transitions (linear conformer) are of negligible probabilities due to large differences of R values corresponding to the NeICl(X, 0, $n_X = 0$) (3.97 Å) and NeICl(A, 13, $n_A \geq 5$) (~ 4.5 Å) states. Franck-Condon transition from the linear NeICl(X, 0, $n_X = 0$) ($R = 3.97$ Å) state occurs inevitable at the repulsive part of the NeICl(A,13,n_A) PES lying much higher than the NeICl(A,13,n_A) dissociation limit. Therefore, according to our data, the strong continuum in Fig. SD3 in the manuscript new version cannot be assigned to the linear conformer.

3.3. Comparison of the calculated and experimental pump-probe and excitation spectra

Comparison of experimental and calculated pump-probe spectra is presented in Fig. 3. The $n_X = 0$, 2 and 1 vdW modes are located in the linear (Ne$^{\cdot}\cdot$I-Cl), antilinear (Ne$^{\cdot}\cdot$l-Cl) and near T-shaped configurations, respectively (see Figs. 1, 2 and Ref. [3]). The low, $n_A = 0-2$, vdW modes are located in near T-shaped configuration, and cannot be populated from the linear $n_X = 0$ mode. Calculations confirm this statement, and experimental pump-probe spectra agree very well (Fig. 3).

Comparison of experimental and calculated NeICl(E, 0, n_E, β, 0, $n_\beta \overset{h\nu_2}{\leftarrow} A$, 13, $n_A = 0$) excitation spectra is presented in Fig. 4. According to the results of calculations, the NeICl(E, 0, $n_E = 0 \leftarrow A$, 13, $n_A = 0$) and NeICl(β, 0, $n_\beta = 0 \leftarrow A$, 13, $n_A = 0$) transitions are the strongest, and this feature corresponds to the probability amplitudes given in Fig. 2. It is impossible to compare calculated FCFs and intensities of experimental excitation bands since laser generation intensity increases with ν_2 value in the $\nu_2 = 22920-23020\,\mathrm{cm}^{-1}$ spectral range, and we have not measured this intensity. Besides, there are power saturation at some bands (see Figs. 4 and 5, *b*). Positions of the calculated and experimental bands are very similar.

3.4. Analysis of the luminescence spectra and population and decay of the NeICl(IP) complexes in the energy range lower than their decay limits

Luminescence spectrum measured at the least wavenumber observed in excitation spectra ($22922.8\,\mathrm{cm}^{-1}$ in Fig. 4) and assigned by us to the NeICl(E, 0, $0 \leftarrow A$, 13, 0) transition is given in Fig. 7, *a*.

We tried to describe the spectrum given in Fig. 7, *a* by luminescence spectra of a free ICl molecule (similar attempts were undertaken for Figs. 7, *b–d*). We have described the $\nu_{\mathrm{lum}}^{\max} \approx 25200\,\mathrm{cm}^{-1}$ band using the ICl(E, $0 \rightarrow X$) luminescence spectrum shifted by $140\,\mathrm{cm}^{-1}$ to the red. To describe the luminescence at the $\nu_{\mathrm{lum}}^{\max} \approx 23000\,\mathrm{cm}^{-1}$ band we have to use the ICl(D', $0 \rightarrow A'$) spectra shifted by $140\,\mathrm{cm}^{-1}$ to the red. However, $140\,\mathrm{cm}^{-1}$ red shift is larger than that obtained from Fig. 6 for NeICl(E), $80\,\mathrm{cm}^{-1}$.

Luminescence spectrum measured at $\nu_2 = 22951.8\,\mathrm{cm}^{-1}$ where the NeICl(D', 0, $n_{D'} \rightarrow A'$ and β, 0, $n_\beta \rightarrow A$) transitions are much stronger than the NeICl(E, $0 \rightarrow X$) one (see Figs. 5 and 7, *b*) are described by the shifted ICl(D', $0 \rightarrow A'$, β, $0 \rightarrow A$) and ICl(E, $0 \rightarrow X$) spectra satisfactorily. One may not say the same about the spectrum measured at $\nu_2 = 22966.3\,\mathrm{cm}^{-1}$ (Fig. 7, *c*) since its low-frequency part cannot be described by the shifted ICl(D', $0 \rightarrow A'$ and β, $0 \rightarrow A$) spectra. As to the spectrum measured at $\nu_2 = 22995.4\,\mathrm{cm}^{-1}$, it is described by the shifted ICl(D', $0 \rightarrow A'$, β, $0 \rightarrow A$) and ICl(E, $0 \rightarrow X$) spectra satisfactorily, again. One sees that the luminescence intensity temporal behaviors depend on excitation wavenumbers (Fig. SD6). Besides, at the $\nu_2 = 22951.8$ and $22966.3\,\mathrm{cm}^{-1}$ bands, maxima of the NeICl(E, 0, $n_E \rightarrow X$) temporal behaviors are shifted to larger time relative to those measured at $\nu_{\mathrm{lum}}^{\max} \approx 23000\,\mathrm{cm}^{-1}$, as it occurs in the case of slow non-adiabatic transitions (see Ref. [29]).

The $E \rightarrow X$ luminescence intensity at the $22951.8\,\mathrm{cm}^{-1}$ and $22966.8\,\mathrm{cm}^{-1}$ bands (Fig. SD 6, *b, c*) is approximately 2% of the total luminescence intensity. Their temporal behavior were obtained by multiple measurements with subsequent averaging and subtraction of the interference signal comparable with the useful signal. Nevertheless, the presented temporal behavior shows a superposition

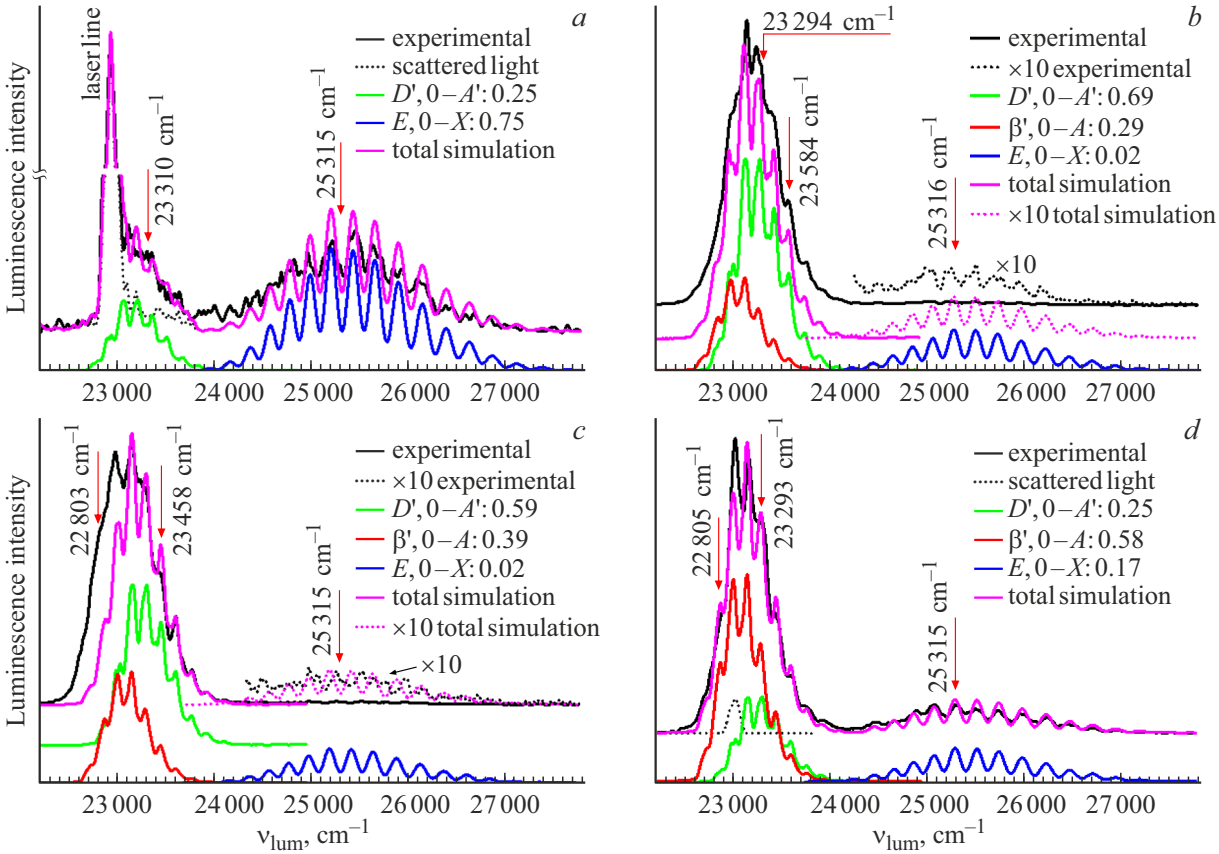

Figure 7. The NeICl(E,0,$n_E \rightarrow X$, D', $0 \rightarrow A'$ and β, 0, $n_\beta \rightarrow A$) luminescence spectra measured at $\nu_2 = 22922.8\,\text{cm}^{-1}$ (*a*), $22951.8\,\text{cm}^{-1}$ (*b*), $22966.3\,\text{cm}^{-1}$ (*c*) and $22995.4\,\text{cm}^{-1}$ (*d*). Spectral resolution is FWHM = 20 Å. Simulations of the NeICl(E, 0, $n_E \rightarrow X$, D', 0, $n'_D \rightarrow A'$ and β, 0, $n_\beta \rightarrow A$) spectra using shifted ICl(E, $0 \rightarrow X$, D', $0 \rightarrow A'$ and β, $0 \rightarrow A$) spectra of a free ICl molecule and branching ratios of the NeICl(E, 0, n_E, D', 0, n'_D and β, 0, n_β) population are given. Luminescence wavenumbers at which temporal behaviors of luminescence intensities have been measured are marked by arrows.

of two processes: (1). $E \rightarrow X$ luminescence (3950 Å) of the mixed $\beta/E/D'$ state, which similar to the time profile of luminescence at wavelengths of 4264 Å ($D' \rightarrow A'$) and 4385 Å (βA). (2). $E \rightarrow X$ luminescence, the main contribution to which comes from the E state populated as a result of NeICl($E/\beta/D'$) collisions with He atoms. To test this assumption, the temporal behaviors were measured at different carrier gas (He) pressures. As the pressure was reduced from 20 to 10 atm, a clear dependence on the He pressure was observed, i.e. the contribution of the luminescence due to collision-induced non-adiabatic transitions (CINATs) was significantly reduced. In the case where the contribution of the E state to the mixed NeICl($E/\beta/D'$) state is large, the contribution of CINATs is small and cannot be observed (Fig. SD6, *a, d*). In Fig. SD6, *b, c*, the time dependences were approximated in the range of 80–140 ns, whereas the laser pulse ends at 50 ns. The longer luminescence decay time compared to the free molecule is due to the „pumping" from the optically populated $\beta/E/D'$ state. The uncertainties in determining the lifetime in this case are higher.

It is worth noting the strong $\nu_2 = 23069.6\,\text{cm}^{-1}$ band in Fig. 4. Luminescence spectrum at this band is similar to that of the transition in the free molecule, ICl($E, 0 \rightarrow X$) (Fig. SD7). However, this band lies in the energy range within the bound part of the NeICl complex, where neither EP nor VP decay of the complex with following luminescence of free ICl($E, 0$) molecules is impossible. Moreover, the radiative lifetime measured at it is 19.7(5) ns and does not correspond to the transition in a free molecule ICl($E, 0 \rightarrow X$), 22.6(2) ns [13]. Therefore, we observe the luminescence of the complex itself. As noted above, luminescence spectra are determined mainly by vibrational structure of the ICl molecule. However, they are shifted because of the difference between vdW part of the PESs belonging to the E and X states. The luminescence spectrum at the $\nu_2 = 23069.6\,\text{cm}^{-1}$ band is not shifted. It can be explained by the features of the wavefunction only. The NeICl($E, 0, n_E$) vdW levels populated at this band lie close to the dissociation limit having the energy $13\,\text{cm}^{-1}$ below it. Wavefunctions are spread over R, Θ coordinates there. As to the NeICl($E, 0, n_{str}, n_b \approx 0$) wavefunctions, they are localized on stretching vdW modes, mainly. At high vdW leves, the probability density is localized at the high R distances predominantly, where PESs of the NeICl(E and X) states are similar. In other words, this is

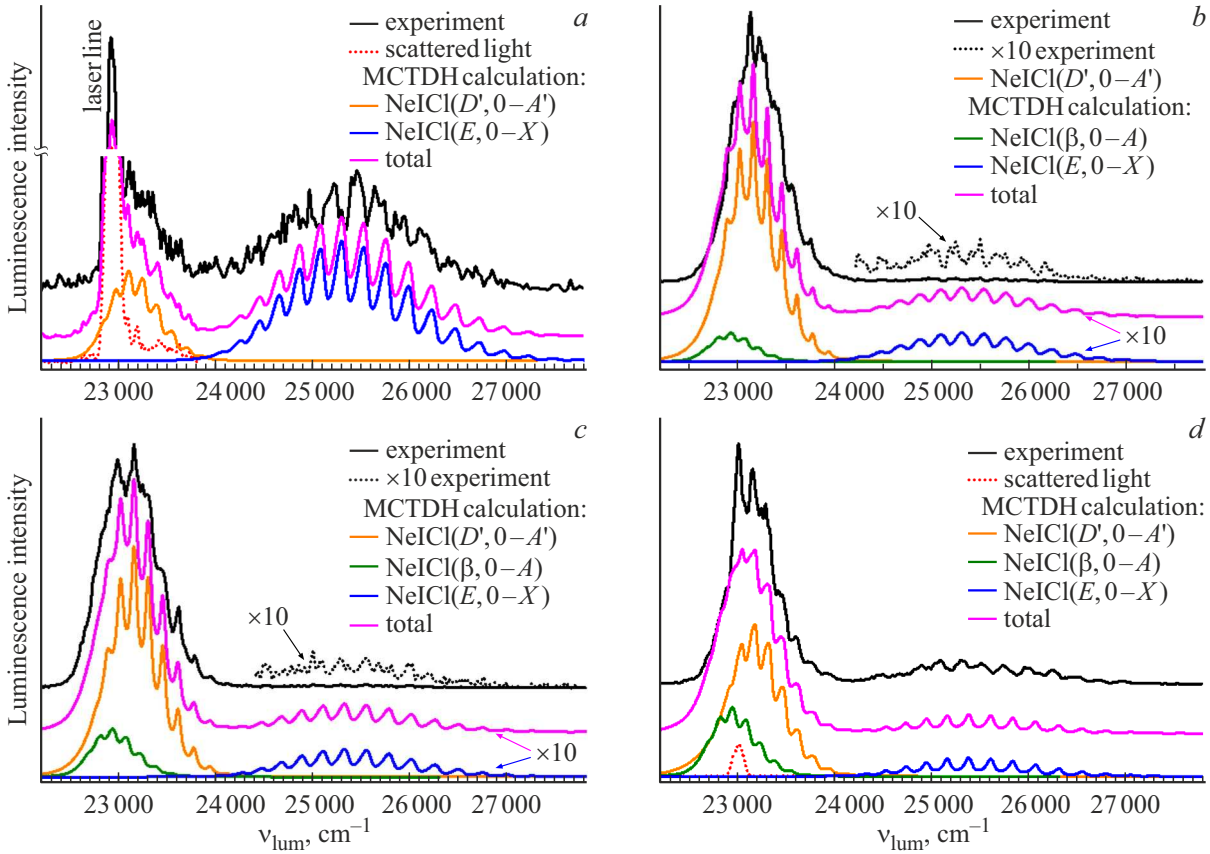

Figure 8. Experimental and calculated using the Heidelberg MCTDH code luminescence spectra of the NeICl(E, 0, n_E, D', 0, n'_D, β, 0, n_β) complexes for $\nu_2 = 22922.8\,\mathrm{cm}^{-1}$ (a), $22951.8\,\mathrm{cm}^{-1}$ (b), $22966.3\,\mathrm{cm}^{-1}$ (c) and $22995.4\,\mathrm{cm}^{-1}$ (d) (see Fig. 4).

a near-dissociation transition where ICl and Ne are almost separated and luminescence spectrum can be the same as the ICl($E \to X$) one at our spectral resolution.

All these features suggest that: (1) the NeICl(E, 0, n_E, D', 0, $n_{D'}$, β, 0, n_β) luminescence spectra cannot be described by shifted spectra of a free molecule; (2) the perturbations in the NeICl(E, 0, n_E, D', 0, $n_{D'}$, β, 0, n_β) complexes depends strongly on their excitation energies.

3.5. Comparison of the experimental and calculated luminescence spectra of complexes

To calculate the luminescence spectra, we used the Heidelberg MCTDH methods [49–51] in the manner described in Ref. [15]. Experimental and calculated luminescence of the NeICl(E, 0, n_E, D', 0, $n_{D'}$) and β, 0, n_β) complexes for $\nu_2 = 22922.8\,\mathrm{cm}^{-1}$ (a), $22951.8\,\mathrm{cm}^{-1}$ (b), $22966.3\,\mathrm{cm}^{-1}$ (c) and $22995.4\,\mathrm{cm}^{-1}$ (d) wavenumbers are given in Fig. 8, a–d.

The $\nu_2 = 22922.8$, $22941.5\,\mathrm{cm}^{-1}$ belong to transitions to the mixed states in which the NeICl(E, 0, $n_E = 0$, 1) states prevail. The $\nu_2 = 22951.8$, $22966.6\,\mathrm{cm}^{-1}$ bands belong to transitions to the mixed states in which the NeICl(β, 0, $n_\beta = 0$, 1) prevail (see Sects. IV.1, IV.4). Nevertheless, the NeICl(D', $0 \to A'$) luminescence prevails at the $\nu_2 = 22951.8$ and $22966.6\,\mathrm{cm}^{-1}$ bands; the similar feature occurs at many other excitation band which have not been analyzed in the paper. There are shifts of calculated spectra relative to the experimental ones. The similar feature has been observed in Ref. [14]. Besides, the NeICl(E, $v_E = 0$, $n_E \to X$, v_X, n_X) spectra correspond to high vX values as in the ICl(E, $v_E = 0 \to X$, v_E) transition (see Ref. [13,15]), while the NeICl(X) PES has been calculated at $r = r_e$. Nevertheless, the calculated luminescence spectrum based on this PES shows reasonable agreement with the experimental data.

3.6. Analysis of the luminescence spectra and population and decay of the NeICl(IP) complexes in the energy range higher than their decay limits

All the bands presented in Fig. 5, a correspond to the energy range in which NeICl(E,1,n_E, D',1,n_D and β, 1, n_β) are populated. Therefore, VP and EP are possible here, and one has to observe luminescence of free ICl(E, 0, D', 0, β, 0) molecules. Experimental data confirm this statement: the spectra are simulated by those of free molecules, and

lifetimes are equal to those of free molecules, also (see Fig. SD8 and Ref. 13).

4. Conclusions

The spectroscopic characteristics of the T-shaped NeICl valence $A1$ and IP $E0^+$, $\beta 1$ states obtained in experiments and calculated using the IDIM PT1 method agree well. Experimental and calculated pump-probe and excitation spectra agree very well. We have observed the $\mathrm{NeICl}(A, v_A, n_A = 0 \overset{h\nu_1}{\leftarrow} X,\ 0,\ n_X = 1)$ and $\mathrm{NeICl}(E,\ v_E,\ \beta,\ v_\beta \overset{h\nu_2}{\leftarrow} A,\ v_A,\ n_A = 0)$ excitation spectra transitions only, in the experiments, and results of calculations agree very well with experimental data. The $\mathrm{NeICl}(E, 0, n_E \rightarrow X)$, $\mathrm{NeICl}(D',\ 0,\ n_{D'} \rightarrow A')$ and $\mathrm{NeICl}(\beta,\ 0,\ n_\beta \rightarrow A)$ luminescence spectra can be satisfactory described by shifted spectra of a free ICl molecule. Nevertheless, these descriptions are incorrect. We have achieved satisfactory descriptions of the $\mathrm{NeICl}(E,\ 0,\ n_E \rightarrow X)$, $\mathrm{NeICl}(D',\ 0,\ n_{D'} \rightarrow A')$ and $\mathrm{NeICl}(\beta,\ 0,\ n_\beta \rightarrow A)$ luminescence spectra using Heidelberg MCTDH method.

Author Declaration

Conflict of Interest

The authors have no conflict to discuss.

Supplementary Material

The Supplementary material includes the $\mathrm{NeICl}(X0^+)$ PES reconstructed based on data of Ref. [3], contour plots of the $\mathrm{NeICl}(A,\ E$ and $\beta)$ PESs, pump-probe, $\mathrm{NeICl}(A,\ 13,\ n_A \leftarrow X,\ 0,\ n_X)$ (pump), $\mathrm{ICl}(E,\ 0 \leftarrow A,\ 13)$ (probe) and $\mathrm{NeICl}(\beta \rightarrow A/D' \rightarrow A')$, $\mathrm{NeICl}(E \rightarrow X)$ luminescence excitation spectra, temporal behaviors of luminescence intensities measured at selected vdW modes, and luminescence spectra of the $\mathrm{NeICl}(E,\ 1,\ D'$,1 and $\beta,\ 1)$ complexes EP and VP products.

References

[1] S. Lukashov, A. Petrov, A. Pravilov. The Iodine Molecule: Insights into Intra- and Intermolecular Perturbation in Diatomic Molecules (Springer, 2018). DOI: 10.1007/978-3-319-70072-4

[2] A. Pravilov. Gas-Phase Photoprocesses (Springer, 2021). DOI: 10.1007/978-3-030-65570-9

[3] R. Prosmiti, C. Cunha, P. Villarreal, G. Delgado-Barrio. J. Chem. Phys. **117** (15), 7017 (2002). DOI: 10.1063/1.1506920

[4] A. Durand, J.C. Loison, J. Vigué. J. Chem. Phys. **106** (2), 477 (1997). DOI: 10.1063/1.474086

[5] O. Roncero, J.A. Beswick, N. Halberstadt, P. Villareal, G. Delgado-Barrio. J. Chem. Phys. **92** (6) 3348 (1990). DOI: 10.1063/1.458578

[6] J.M. Skene, J.C. Drobits, M.I. Lester. J. Chem. Phys. **85** (4), 2329−2331 (1986). DOI: 10.1063/1.451080

[7] A.B. McCoy, J.P. Darr, D.S. Boucher, P.R. Winter, M.D. Bradke, R.A. Loomis. J. Chem. Phys. **120** (6) 2677 (2004). DOI: 10.1063/1.1636693

[8] D.B. Strasfeld, J.P. Darr, R.A. Loomis. Chem. Phys. Letts. **397** (1) 116 (2004). DOI: :10.1016/j.cplett.2004.08.083

[9] T.A. Stephenson. J. Chem. Phys. **97** (9) 6262 (1992). DOI: 10.1063/1.463688

[10] T.A. Stephenson, Y. Hong, M.I. Lester. J. Chem. Phys. **94** (6) 4171 (1991).

[11] J.P. Darr, R.A. Loomis. J. Chem. Phys. **129** (14), 144306 (2008). DOI: 10.1063/1.2990661

[12] J.C. Drobits, M.I. Lester. J. Chem. Phys. **86** (4) 1662 (1987). DOI: 10.1063/1.452164

[13] V.V. Baturo, S.S. Lukashov, S.A. Poretsky, A.M. Pravilov, M.M. Sivokhina. Chem. Phys. Letts. **765** (1) 138259 (2021). DOI: 10.1016/j.cplett.2020.138259

[14] S.A. Poretsky, A.M. Pravilov. Mol. Phys. **120**, e1955166 (2021), DOI: 10.1080/00268976.2021.1955166

[15] S.S. Lukashov, I.I. Martynov, S.A. Poretsky, A.M. Pravilov, M.M. Sivokhina. J. Chem. Phys. **157** (16) 164302 (2022). DOI: 10.1063/5.0109849

[16] V.V. Baturo, S.S. Lukashov, S.A. Poretsky, A.M. Pravilov. Chem. Phys. Letts. **696** (1), 26 (2018). DOI: 10.1016/j.cplett.2018.02.031

[17] A.A. Buchachenko, N. Halberstadt, B. Lepetit, O. Roncero. Int. Rev. Phys. Chem. **22** (1) 153 (2003). DOI: 10.1080/0144235031000075726

[18] V.V. Baturo, I.N. Cherepanov, S.S. Lukashov, S.A. Poretsky, A.M. Pravilov. Chem. Phys. Letts. **647**, 161−164 (2016). DOI: 10.1016/j.cplett.2016.01.053

[19] V.V. Baturo, S.S. Lukashov, S.A. Poretsky, A.M. Pravilov, A.I. Zhironkin. Chem. Phys. Letts. **662** (1) 250 (2016). DOI: 10.1016/j.cplett.2016.09.021

[20] V.V. Baturo, R. Kevorkyants, S.S. Lukashov, S.A. Poretsky, A.M. Pravilov, A.I. Zhironkin. Chem. Phys. Letts. **684** (1) 357 (2017). DOI: 10.1016/j.cplett.2017.07.007

[21] V.V. Baturo, S.S. Lukashov, S.A. Poretsky, A.M. Pravilov. Eur. Phys. J. D **71**, 217 (2017). DOI: 10.1140/epjd/e2017-80142-6

[22] V.V. Baturo, R. Kevorkyants, S.S. Lukashov, S.S. Onishchenko, S.A. Poretsky, A.M. Pravilov. Chem. Phys. Letts. **714** (1) 213 (2019). DOI: 10.1016/j.cplett.2018.10.084

[23] V.V. Baturo, S.S. Lukashov, S.A. Poretsky, A.M. Pravilov. J. Phys. B: At. Mol. Opt. Phys. **52**, 145101 (2019). DOI: 10.1088/1361-6455%2Fab2496

[24] V.V. Baturo, S.S. Lukashov, S.A. Poretsky, A.M. Pravilov, A.I. Zhironkin. J. Phys. B: At. Mol. Opt. Phys. **53**, 035101 (2020). DOI: 10.1088/1361-6455/ab582b

[25] A.S. Andreev, V.V. Baturo, S.S. Lukashov, S.A. Poretsky, A.M. Pravilov, A.I. Zhironkin. J. Chem. Phys. **152** (23) 234307 (2020). DOI: 10.1063/5.0008760

[26] S.S. Lukashov, I.I. Martynov, S.A. Poretsky, A.M. Pravilov, M.M. Sivokhina. ChemPhysChem 24, e202300274 (2023). DOI: 10.1002/cphc.202300274

[27] A.M. Pravilov. Radiometry in Modern Scientific Experiments (Springer, Wien New-York, 2011). DOI: 10.1007/978-3-7091-0104-9

[28] M.E. Akopyan, V.V. Baturo, S.S. Lukashov, S.A. Poretsky, A.M. Pravilov. J. Phys. B. Atom. Molec. and Optic. Phys. **44**, 205101 (2011). DOI: 10.1088/0953-4075/44/20/205101

[29] M.E. Akopyan, V.V. Baturo, S.S. Lukashov, S.A. Poretsky, A.M. Pravilov. Chem. Phys. **462**, 3 (2015). DOI: 10.1016/j.chemphys.2015.08.014

[30] J.A. Coxon, M.A. Wickramaaratchi. J. Molec. Spectrosc. **79** (2) 380 (1980). DOI: 10.1016/0022-2852(80)90220-9
[31] H.G. Hedderich, P.F. Bernath, G.A. McRae. J. Molec. Spectrosc. **155** (2), 384 (1992). DOI: 10.1016/0022-2852(92)90527-U
[32] J.C.D. Brand, A.R. Hoy, S.M. Jawant. J. Molec. Spectrosc. **106** (2) 388 (1984). DOI: 10.1016/0022-2852(84)90169-3
[33] R.J. Donovan, T. Ridley, K.P. Lawley, P.J. Wilson, Chem. Phys. Letts. **205** (3, 4) 129 (1993). DOI: 10.1016/0009-2614(93)89216-5
[34] J.C.D. Brand, D. Bussiéres, A.R. Hoy, S.M. Jawant, D.B. Miller, Opt. Comm. **48**, 195 (1983). DOI: 10.1016/0030-4018(83)90084-6
[35] D. Bussiéres, A.R. Hoy. Can. J. Phys. **62** (12) 1941 (1984). DOI: 10.1139/p84-237
[36] B.L. Grigorenko, A.V. Nemukhin, A.A. Buchachenko, N.F. Stepanov, S.Y. Umanskii. J. Chem. Phys. **106** (11), 4575 (1997). DOI: 10.1063/1.473499
[37] B. Schmidt and U. Lorenz. Comput. Phys. Commun. **213**, 223 (2017). DOI: 10.1016/j.cpc.2016.12.007
[38] K.C. Janda, C.R. Bieler, in Atomic and Molecular Clusters, ed. by I.R. Bernstein (Elsevier, Amsterdam), 455 (1990).
[39] J.I. Cline, N. Sivakumar, D.D. Evard, C.R. Bieler, B.P. Reid, N. Halberstadt, S.R. Hair, K.C. Janda. J. Chem. Phys. **90** (5), 2605(1989). DOI: 10.1063/1.456669
[40] J.C. Drobits, M.I. Lester. J. Chem. Phys. **88** (1), 120 (1988). DOI: 10.1063/1.454644
[41] J.C. Drobits, M.I. Lester. J. Chem. Phys. **89** (8), 4716 (1988), DOI: 10.1063/1.455735
[42] C.D. Withers, T.G. Wright, L.A. Viehland, L. Grossman, C.C. Kirkpatrick, E.P.F. Lee. J. Chem. Phys. **135** (2) 024312 (2011). DOI: 10.1063/1.3598472
[43] I. Last, T.F. George. J. Chem. Phys. **87** (2), 1183 (1987). DOI: 10.1063/1.453298
[44] A.A. Buchachenko, T.V. Tscherbul, J. Kłos, M.M. Szcześniak, G. Chałasiński, R. Webb, L.A. Viehland. J. Chem. Phys. **122** (19), 194311 (2005). DOI: 10.1063/1.1900085
[45] S.A. Poretsky, A.M. Pravilov, M.M. Sivokhina, Chem. Phys. Letts. **829**, 140753 (2023). DOI: 10.1016/j.cplett.2023.140753
[46] M.D. Havey, J.J. Wright. J. Chem. Phys. **68** (10), 4754 (1968). DOI: 10.1063/1.435543
[47] J.P. Darr, R.A. Loomis, Faraday Disc. **127**, 213 (2004). DOI: 10.1039/B316117J
[48] D.S. Boucher, M.D. Bradke, J.P. Darr, R.A. Loomis, J. Phys. Chem. A, **107** (36), 6901 (2003). DOI: 10.1021/jp035284z
[49] H.D. Meyer, U. Manthe, and L.S. Cederbaum, Chem. Phys. Lett. **165** (1), 73 (1990). DOI: 10.1016/0009-2614(90)87014-I
[50] M.H. Beck, A. Jäckle, G.A. Worth, H.D. Meyer, Phys. Rep. **324** (1), 1 (2000). DOI: 10.1016/S0370-1573(99)00047-2
[51] G.A. Worth, M.H. Beck, A. Jäckle, H.-D. Meyer. The MCTDH Package, Version 8.2, (2000). H.-D. Meyer, Version 8.3 (2002), Version 8.4 (2007). O. Vendrell, H.-D. Meyer Version 8.5 (2013). Versions 8.5 and 8.6 contain the ML MCTDH algorithm. See http://mctdh.uni-hd.de for a description of the Heidelberg MCTDH package.